Supporting information

Simultaneous removal of Pb^{2+} and direct red 31 dye from contaminated water using *N-(2-hydroxyethyl)-2-oxo-2H-chromene-3-carboxamide* loaded chitosan nanoparticles

Mehrez E. El-Naggar [a*], Emad K. Radwan [b**], Huda R. M. Rashdan [c], Shaimaa T. El-Wakeel [b], Asmaa A. Koryam [b], Ahmed Sabt [d]

[a] Institute of Textile Research and Technology, National Research Centre, 33 El Buhouth St, Dokki, Giza, 12622, Egypt.

[b] Water Pollution Research Department, National Research Centre, 33 El Buhouth St, Dokki, 12622 Giza, Egypt.

[c] Chemistry of Natural and Microbial Products Department, Pharmaceutical and Drug Industries Research Institute, National Research Centre, 33 El Buhouth St, Dokki, 12622 c

[d] Department of Natural Compounds Chemistry, Pharmaceutical and Drug Industries Research Institute, National Research Centre, 33 El Buhouth St, Dokki, 12622 Giza, Egypt.

Corresponding authors.

[*] Mehrez E. El-Naggar; mehrez_chem@yahoo.com

[**] Emad K. Radwan emadk80@gmail.com

Contents

Material and methods

Chemicals.

Salicylaldehyde 98%, diethyl malonate 99%, piperidine 99%, absolute ethanol, ethanolamine 99%, chitosan and sodium tripolyphosphate were purchased from Sigma-Aldrich (USA). Glacial acetic acid was obtained from across co. (Germany). All chemicals were used as received without purification.

Characterization techniques.

All melting points were determined by an electrothermal apparatus and are uncorrected. ^{1}H- NMR and ^{13}C-NMR spectra of compound **4** were recorded in $(CD_3)_2SO$ solutions by a BRUKER 500 FT-NMR system spectrometer, and chemical shifts were expressed in ppm units using TMS as an internal reference. The as-prepared CsNP and C@CsNPs nanocomposites were characterized as follows: Field emission scanning electron microscopy (FESEM, S 4800; Hitachi, Japan) and transmission electron microscopy (TEM; JEOL USA, Inc, Japan) were used to examine the morphology of CsNPs, C1@CsNPs and C2@CsNPs. The SEM was operated at a 15 kV acceleration voltage. While, for the TEM analysis each sample was placed on a carbon-coated grid and the instrument was set to 200 kV. Particle size analyzer and polydispersity index were assessed using dynamic light scattering (DLS) technique by a Nano-ZS Zetasizer, Malvern Instruments, UK. Each liquid sample was deposited in a folded capillary cell in the instrument holder with no air bubbles. CsNPs, C1@CsNPs, and C2@CsNPs colloidal liquid injectable formulations were characterized using standard procedures in accordance with Malvern instruments' manual instructions. Fourier transform infrared spectroscopy (FTIR; Perkin-Elmer, Monza, Italy) was utilized to examine the functional groups of compound **4**, CsNPs and C2@CsNPs in the frequency range 4000–400 cm^{-1}, the spectra were collected as an average of 32 scans with a resolution of 2 cm^{-1}.

Analysis of adsorption data.

The removal percentage (R%) was calculated by Eq. S1, while the amount of adsorptive uptake per unit mass of adsorbent at any time t (q_t) was calculated according to Eq. S2.

$$\mathrm{R}\ (\%) = \left(1 - \frac{C_t}{C_o}\right) \times 100 \qquad \text{(S1)}$$

$$q_t = (C_o - C_t)\frac{V}{m} \qquad \text{(S2)}$$

where C_o (mg/L) is the initial concentration of adsorptive, C_t (mg/L) is the residual concentration of adsorptive at time t and converts to C_e (mg/L) at equilibrium state, V (L) is the volume of adsorptive solution, and m (g) is the mass of adsorbent.

Analysis of adsorption kinetic data.

The kinetic data was analyzed by Lagergren pseudo-first-order (PFO) [1], pseudo-second-order (PSO) [2], and Elovich [3] equations. Both ***PFO*** and ***PSO*** models are based on assuming that the adsorption process is driven by the difference between the average adsorptive uptake q_t and the equilibrium adsorptive uptake q_e. The difference between the two models is that in the PFO the overall adsorption rate is proportional to the driving force while in the PSO the overall adsorption rate is proportional to the square of the driving force. On the other hand, ***Elovich*** equation is an empirical equation that assume energetically heterogeneous adsorbent surface and has been widely applied to chemisorption data.

PFO $$q_t = q_e\,(1 - e^{-k_1 t}) \qquad \text{(S3)}$$

PSO $$q_t = \frac{k_2 q_e^2 t}{1 + k_2 q_e t} \qquad \text{(S4)}$$

Elovich $$q_t = \frac{1}{\beta}\ln(1 + \alpha\beta t) \qquad \text{(S5)}$$

where q_e is the amount of adsorptive uptake per unit mass of adsorbent at equilibrium state, k_1 (1/min) and k_2 (g/mg min) are the rate constants of the PFO and PSO, respectively, α (mg/g min) is the initial adsorption rate, and β is related to the extent of surface coverage and activation energy (g/mg).

Analysis of adsorption equilibrium data.

The equilibrium data was analyzed using two-parameter (Freundlich [4], Langmuir [5], Temkin [6], and Dubinin–Radushkevich (D–R) [7]) and three-parameter models (Redlich–Peterson (R–P) [8], and Sips [9]) Eqs. S6-S12.

Two-parameter isotherm models.

Freundlich model is based on the assumption that the adsorbent surface is heterogeneous and the adsorption process is not restricted to monolayer formation. The exponent of Freundlich model

describes the heterogeneity of the surface, and the exponential distribution of the adsorption sites and their energies [4].

Freundlich $$q_e = k_F C_e^{1/n_F} \quad \text{(S6)}$$

Langmuir $$q_e = \frac{q_L k_L C_e}{1 + k_L C_e} \quad \text{(S7)}$$

$$R_L = \frac{1}{1 + k_L\, C_o} \quad \text{(S8)}$$

Temkin $$q_e = \left(\frac{\mathrm{RT}}{b_T}\right) ln A_T C_e \quad \text{(S9)}$$

D–R $$q_e = q_{D\text{-}R}\, e^{\left[-\beta\left(\mathrm{RT}\ln\left(1+\frac{1}{C_e}\right)\right)\right]} \quad \text{(S10)}$$

R–P $$q_e = \frac{k_{R\text{-}p}\, C_e}{1 + a_{R\text{-}P}\, C_e^g} \quad \text{(S11)}$$

Sips $$q_e = \frac{q_S\, k_S\, C_e^{n_S}}{1 + k_S\, C_e^{n_S}} \quad \text{(S12)}$$

where q_L, $q_{D–R}$, and q_S (mg/g) are the Langmuir, D–R and R–P maximum adsorption capacity, respectively, k_L and k_S (L/mg) are the Langmuir and Sips equilibrium constant, respectively, k_F ($mg^{(1-1/n)}L^{(1/n)}/g$) is Freundlich constant, n_F, g, and n_S (–) are Freundlich, R–P and Sips exponent, respectively, β (mol^2/J^2) is D–R constant related to the mean free energy of adsorption, R is the universal gas constant, T (K) is the absolute temperature, b_T (KJ/mol) is Temkin constant related to the heat of adsorption, A_T (L/g) is Temkin equilibrium binding constant, $k_{R–P}$ (L/mg) is R–P constant related to the adsorption capacity, and $a_{R–P}$ (L/mg) is R–P constant related to the affinity of the binding sites.

Contrary to Freundlich, ***Langmuir model*** is based on the assumption that the adsorbent surface has identical energetically equal definite localized adsorption sites that can capture one layer only of the adsorbate with one molecule thickness [5]. The separation factor (R_L) is an essential character of Langmuir model that describe the adsorption nature. It can be represented by Eq. S8.

Dubinin–Radushkevich (D–R) model is more general than Langmuir and Freundlich. It assumes a pore filling mechanism and multilayer character which involve Van der Waal's forces. D–R is commonly used to physisorption processes [7].

Temkin model takes account of the interactions between the adsorbent and adsorbate at intermediate concentration range and assumes a linear decrease of the heat of adsorption with the surface coverage and a uniform distribution of binding energies [6]. The characteristic feature of Temkin model is that it enables the calculation of the heat of adsorption.

Three-parameter isotherm models.

Redlich–Peterson (R–P) model [8] is a hybrid empirical model that combines the features of both Langmuir and Freundlich. It can be applied over a wide range of concentrations to both homogeneous and heterogeneous systems.

Sips model [9] is another combined form of Langmuir and Freundlich that can predicts the adsorption on heterogenous surface and overcomes the limitation of Freundlich model at high adsorptive concentration. Sips model is reduced to Freundlich model at low adsorptive concentrations and to Langmuir model at high adsorptive concentrations.

Criteria for selecting the best fitting model.

The quality and accuracy of fitting of the kinetic and isotherm models to the data from experimentations was evaluated using three common statistical parameters, specifically, coefficient of determination (R^2), nonlinear chi-square (χ^2), and root-mean-square deviation (RMSD), Eqs. S13-S15.

$$R^2 = \frac{\sum \left(q_{e,cal} - \bar{q}_{e,exp}\right)^2}{\sum \left(q_{e,cal} - \bar{q}_{e,exp}\right)^2 - \sum \left(q_{e,cal} - q_{e,exp}\right)^2} \quad \text{(S13)}$$

$$\chi^2 = \sum_{i=1}^{N} \left[\frac{\left(q_{e,exp} - q_{e,cal}\right)^2}{q_{e,cal}}\right] \quad \text{(S14)}$$

$$RMSD = \sqrt{\frac{1}{N-M}\sum_{i=1}^{N}(q_{e,measured} - q_{e,model})^2} \quad \text{(S15)}$$

A value of R^2 close to unity and values of χ^2 and RMSD close to zero indicate that the fitting model almost equals the actual data. Another important criterion is that the value of the calculated parameters of the model should be realistic and meaningful [10].

Binary adsorption

The effect of the interaction between DR31 and Pb^{2+} was evaluated by calculating the P-factor (P_f) which is the ratio of the amount of an adsorbate per unit mass of the adsorbent in the binary ($q_{b,i}$) and unary ($q_{s,i}$) system (Eq. S16) under identical conditions.

$$P_{f,i} = \frac{q_{b,i}}{q_{u,i}} \tag{S16}$$

Figures

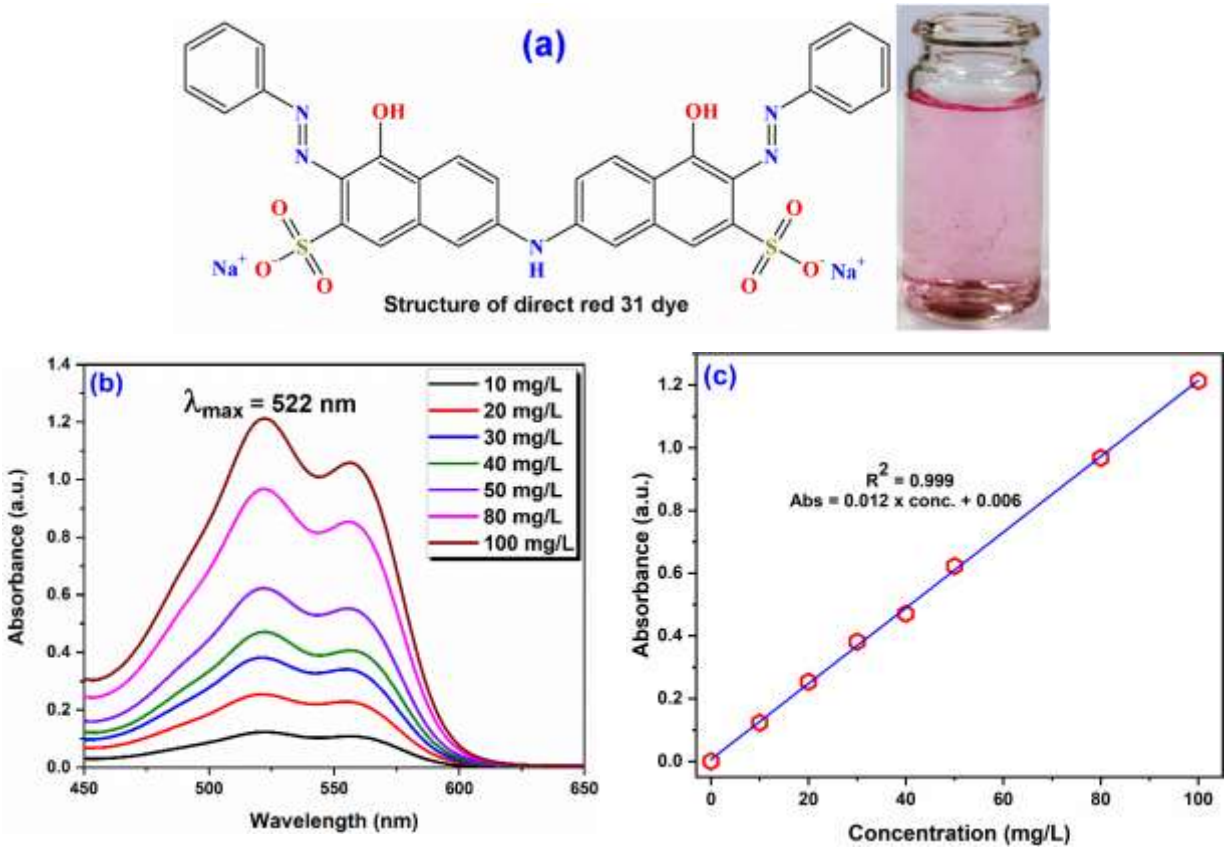

Figure S1. Structure and digital picture (a), visible spectrum (b), and calibration curve (c) of DR 31 dye.

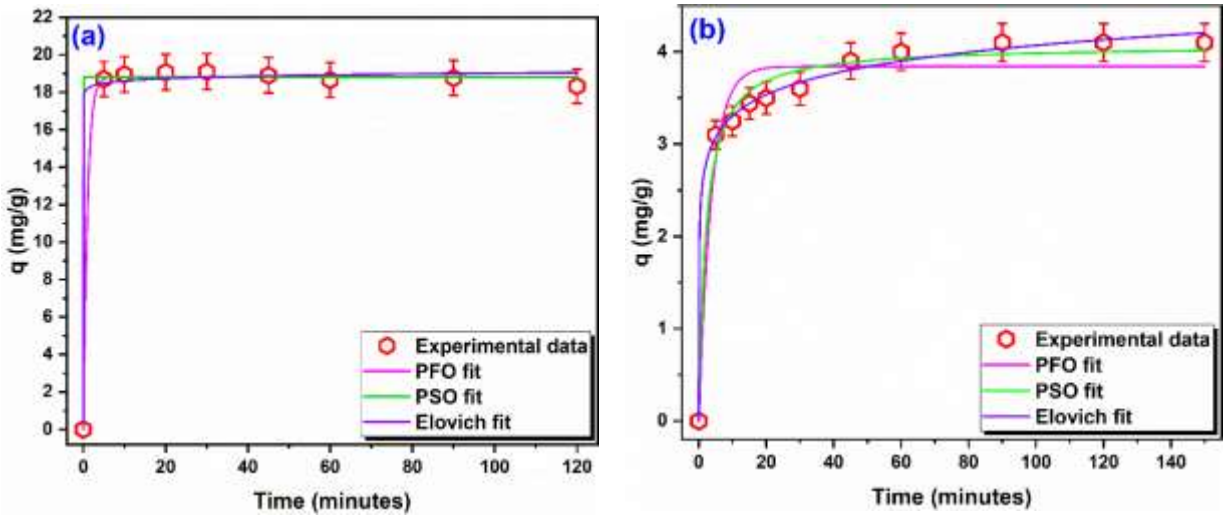

Figure S2. Adsorption kinetics and fitted kinetic models for (a) DR31 dye (pH_o 3, C_o 10 mg/L, dosage 0.50 g/L) and (b) Pb^{2+} (pH_o 5.5, C_o 10 mg/L, dosage 2.00 g/L) onto C1@CsNPs.

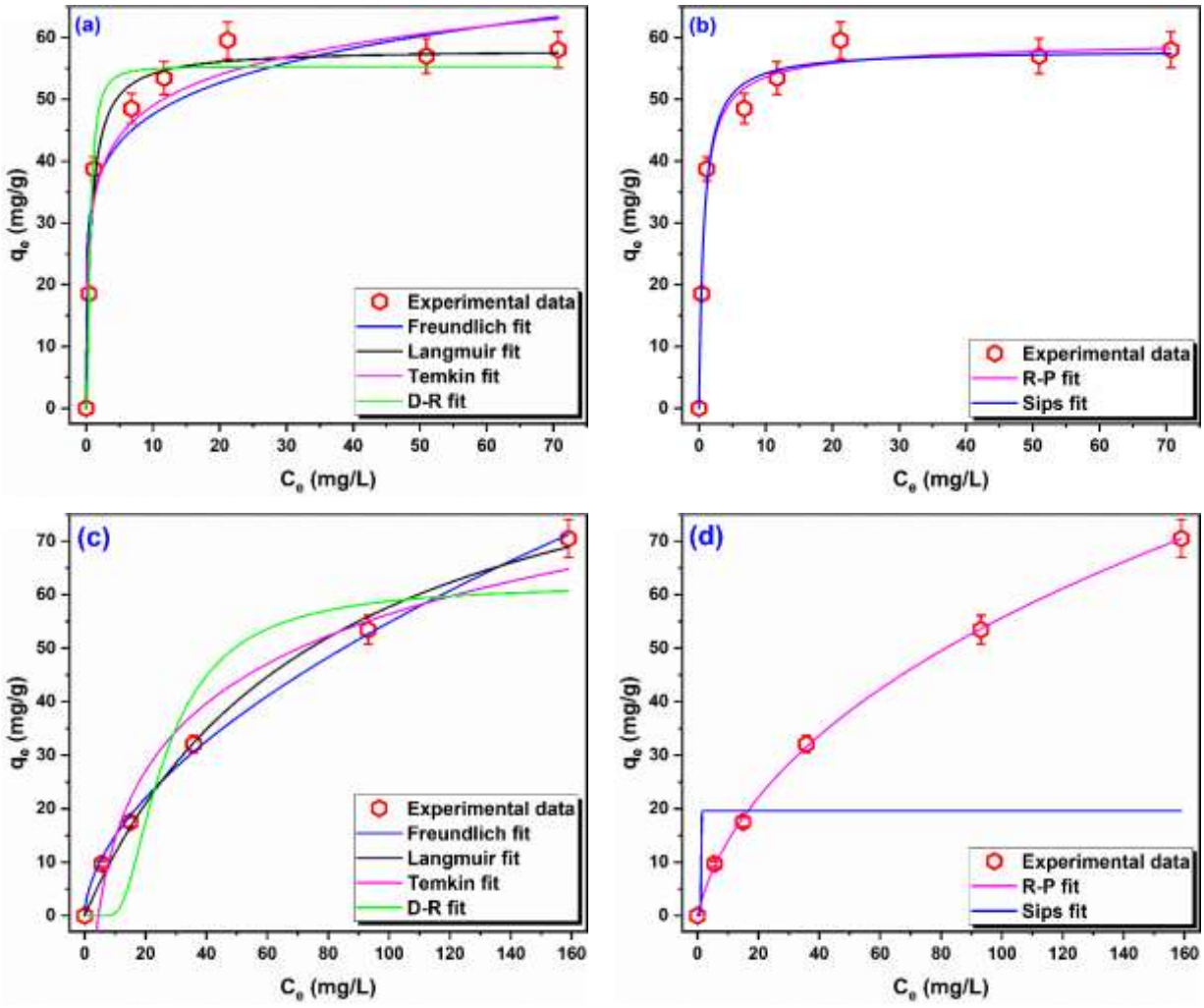

Figure S3. Experimental adsorption isotherm and fitted two- and three-parameter isotherm models for DR31 (pH_o 3, contact time 1 hr, dosage 0.50 g/L) (a) and (b), and Pb^{2+} (pH_o 5.5, contact time 2 hr, dosage 2.00 g/L) (c) and (d), respectively.

References

1. S. Langergren and B. K. Svenska, *Veternskapsakad Handlingar*, 1898, **24**, 1-39.
2. G. Blanchard, M. Maunaye and G. Martin, *Water Research*, 1984, **18**, 1501-1507.
3. S. Roginsky and Y. B. Zeldovich, *Acta Phys. Chem. USSR*, 1934, **1**, 2019.
4. H. M. F. Freundlich, *Journal of Physical Chemistry*, 1906, **57**, 385-470.
5. I. Langmuir, *Journal of the American Chemical society*, 1918, **40**, 1361-1403.
6. M. I. Temkin and V. Pyzhev, *Acta Physiochim* 1940, **URSS 12**, 327-356.
7. M. M. Dubinin and L. V. Radushkevich, *Proc. Acad. Sci. USSR Phys. Chem. Sect.* , 1947, **55**, 331-337.
8. O. Redlich and D. L. Peterson, *Journal of Physical Chemistry*, 1959, **63**, 1024-1024.
9. R. Sips, *J. Chem. Phys*, 1948, **16**, 490-495.
10. M. A. Al-Ghouti and D. A. Da'ana, *Journal of Hazardous Materials*, 2020, **393**, 122383.